ASIAN JOURNAL OF CIVIL ENGINEERING (BHRC) VOL. 15, NO. 5 (2014)
PAGES 633-653

STRUCTURAL GEOMETRICAL NONLINEAR ANALYSIS BY DISPLACEMENT INCREMENT

M. Rezaiee-Pajand*, M. Salehi-Ahmadabad and M. Ghalishooyan
Department of Civil Engineering, Ferdowsi University of Mashhad, Mashhad, Iran

Received: 10 February 2014; **Accepted:** 3 May 2014

ABSTRACT

This study is devoted to tracing the equilibrium path of structures with severe nonlinear behavior. A new displacement increment is suggested to do the analysis. Moreover, the increment of the load factor is obtained by minimizing the residual displacement. To evaluate the capabilities of the presented method against existing ones, a comparison study is performed. In this process, five benchmark frame and truss problems are solved. Each of the structures is analyzed more than 600 times, and the outcomes are compared with each other. According to the results, the authors' scheme is more competent than the methods of residual load minimization, normal plane, updated normal plane, cylindrical arc length, work control, residual displacement minimization, generalized displacement control and modified normal flow.

Keywords: Displacement increment; nonlinear analysis; numerical stability; nonlinear solution techniques; equilibrium path; load factor.

1. INTRODUCTION

Due to the great importance of the structural nonlinear analysis, researchers have always been looking for capable schemes to achieve the nonlinear equilibrium path. These strategies should be efficient enough to traverse the various snap-through, snap-back and buckling points of all equilibrium states. This characteristic should especially be taken into account for the structures with intense nonlinear behavior. So far, a variety of tactics have been proposed, which are capable and efficient for solving nonlinear problems. Traditional and old procedures are not able to achieve the severe nonlinear equilibrium path and diverge in passing limit points. It is worth mentioning that researchers have not yet obtained a method which can trace all types of load-deflection curves. In other words, the most efficient techniques of nonlinear structural analysis fail in some cases, and the intervention of the analyst is necessary during the solution process.

*E-mail address of the corresponding author: rezaiee@um.ac.ir (M. Rezaiee-Pajand)

It should be pointed out that the traditional approaches, such as, pure increment [1,2], Newton-Raphson, modified Newton-Raphson, displacement control [3] and its modified versions [4-6], have less capability compared with the advanced ones. This disadvantage may appear in the case of not passing the load limit points for Newton-Raphson and modified Newton-Raphson methods [4,7-9], not passing the displacement limit points for displacement control technique [7,10,11], having high cost and analysis time, having low convergence rate and increasing drift-off error from the equilibrium path for the pure incremental approach. The following is a brief history of the advanced nonlinear solution schemes.

In 1980, Bergan calculated the load increment in each iteration and proposed the residual load minimization technique by minimizing the difference between the load applied on structure and its internal force [12]. Other capable nonlinear analysis approaches are called arc length method. For the first time, this procedure was suggested by Wempner [13] and Riks [14, 15]. After that, these schemes were widely employed and developed by other researchers [7, 10, 16-18]. In 1981, Crisfield formulated the cylindrical arc length strategy and called it the modified Riks approach [10]. In the normal plane arc length technique, the locus of the iteration points is perpendicular to the tangent passes through the prior equilibrium point [7, 15]. If the perpendicular process is repeated in each iterative step, then the algorithm is called updated normal plane [7, 19, 20].

In 1981 and 1985, the constant work control technique was used by assuming that the work increment is constant [8, 21]. After the Newton-Raphson method, which is unable to pass the load limit points on the equilibrium path, researchers presented various approaches for overcoming this difficulty. The arc length strategy of Crisfield [10], Riks [14, 15] and Ramm [7], the displacement control [4-6] and the constant work control of Powell and Simons [8] and Yang [6] were not efficient in some cases. On the other hand, these techniques do not follow the shortest path to find the equilibrium points. In 1988, the residual displacement minimization tactic was proposed by Chan [22]. Following that, Yang and Shieh suggested the generalized displacement control approach in 1990 [23]. In 2008, the modified form of the normal flow algorithm [25, 26] was proposed by Saffari et al. [24].

Structural nonlinear solvers have been developed extensively in the last few decades. As it has been described so far, the literature on this subject is not very limited. In a recent attempt, based on the Newton–Raphson algorithm, a two-point method was presented in 2011 [27]. This tactic worked as a predictor–corrector one, most frequently taking Newton's method in the first iteration. In spite of the fact, the presented procedure was faster than the classic Newton–Raphson algorithm; it had the problem of passing limit points. In 2012, Mansouri and Saffari proposed an efficient function for reducing the computing time and number of iterations in the Newton–Raphson method coupled with the two-point methodology [28]. They performed the nonlinear analysis of planar frames, and reduced the computing time and also the number of iterations, compared with the classic Newton–Raphson algorithm. It is well known noted that Newton–Raphson scheme, and all related techniques cannot pass the limit points of displacement curves. To broadly examine the solution techniques' abilities for the structures with geometrical nonlinear behavior, formulations of several famous approaches were presented by Rezaiee-Pajand, et al. [29]. Moreover, other features of these approaches and their algorithms for tracing of the structural equilibrium path were also investigated. In the second part of the mentioned study,

robustness and efficiency of the solution tactics were comprehensively evaluated by performing numerical analyses [30]. In this investigation, criteria such as, number of diverged and complete analyses, the ability of passing load limit and snap-back points, the total number of steps and iteration process, the analysis running time and divergence points were extensively examined. Furthermore, capabilities and deficiencies of each solver, in comparison with the other ones, were discussed and finally superior solution schemes were introduced. In another event, a functionally graded plate was analyzed for both thermal and mechanical loadings by Phung-Van et al. [31]. A cell-based smoothed three-node Mindlin plate element was modeled to find geometrically nonlinear solution. In this study, the higher-order shear deformation plate theory was considered. A two-step procedure was utilized, including a step of analyzing the temperature field along the thickness of the structure, and another step for solving the geometrically nonlinear behavior.

By reviewing nonlinear solution procedures of the structures, it will be evident that a very significant issue of the numerical instability still exists in these solution strategies. The main purpose of the authors' algorithm is preventing the divergence of nonlinear solution from the load limit and snap-back points. In this paper, a new displacement increment is proposed for tracing the equilibrium path of structures. If this formulation and also the load factor increment of the residual displacement minimization are used simultaneously, remarkable results can be obtained. These outcomes show that the presented approach has a good numerical stability in solving the structures with severe nonlinear behavior. This merit will be clarified in comparison study with the abilities of the other advanced procedures.

In the coming lines, the proposed formulation is first addressed. Afterwards, different problems are solved by this technique, and the results are compared with the other advanced solvers. In this procedure, the ability of the authors' technique is demonstrated against the residual load minimization, the normal plane, the updated normal plane, the cylindrical arc length, the residual displacement minimization and the generalized displacement control and also the modified normal flow methods.

2. THE PROPOSED DISPLACEMENT INCREMENT

To find the behavior of structure, there is a need to solve the governing equilibrium equations in the load-displacement space. These equations can be written as follows:

$$f(u,\lambda)=0 \tag{1}$$

Parameters λ and u show the scalar load factor and the displacement vector of structure, respectively. Tracing the equilibrium path of a structure with N degrees of freedom is done in a N+1-dimension space. Therefore, another constraint, like the below one, must be utilized to analyze structure and find all unknowns:

$$f^{*}(u,\lambda)=0 \tag{2}$$

In order to solve the governing system of equations for the structures with nonlinear

behavior, incremental-iterative strategy can be used. In these techniques, the following equations are employed:

$$\left[\frac{\partial f}{\partial \lambda}\frac{\partial f}{\partial u}\right]\begin{bmatrix}\delta\lambda\\ \delta u\end{bmatrix}=-f \tag{3}$$

Where, $\delta\lambda$ and δu are the load factor increment and the displacement increment in the iteration stages, respectively. Researchers have proposed various techniques in order to calculate the displacement increment and the load factor for tracing the nonlinear equilibrium path of structure. Watson et al. employed the normal flow algorithm in order to solve the governing equation of structures' nonlinear behavior [25, 26]. Based on the mentioned algorithm, the displacement increment in corrector step is obtained by the minimum norm solution of Eq.3, in the following form.

$$\delta u = V - \frac{V^T \delta u^*}{\delta u^{*T} \delta u^*}\delta u^* \tag{4}$$

Here, the answer V is found by employing an arbitrary constraint. It should be noted that the vector V is a particular solution for Eq.3. The parameter δu^* shows the incremental vector of displacement. Although Eq.3 has infinite answers, its minimum norm solution is unique, because the iterative steps move on the shortest path or the normal path until reaching the equilibrium curve of the structure [32]. Thus, the iterative analyses are performed along the lines normal to the Davidenko's flow curve until achieving the equilibrium point [33]. Fig. 1 illustrates Davidenko's flow curve and the equilibrium paths. It should be mentioned that the equation of the Davidenko's flow lines, utilizing perturbation parameter η, is written as follows:

$$f(u,\lambda)=\eta \tag{5}$$

By changing the parameter η, a set of curves is obtained, which are known as the Davidenko's flow curves [33]. Fig. 1 presents the mentioned solution process. Based on Fig. 2, the displacement increment can be determined by the linear equation of Batoz and Dhatt [4]:

$$\delta u_i^n = \delta\lambda_i^n \delta u_i'^n + \delta u_i''^n \tag{6}$$

where, $\delta u_i'^n$ is the displacement increment due to the reference load. The displacement increment $\delta u_i''^n$ is also caused by the residual load. These parameters are illustrated in Fig. 2. The superscript n is used here to denote the analysis step number and the subscript *i* indicates the iterative cycle i within the analysis step n. The mentioned displacement increments are obtained by the following equations:

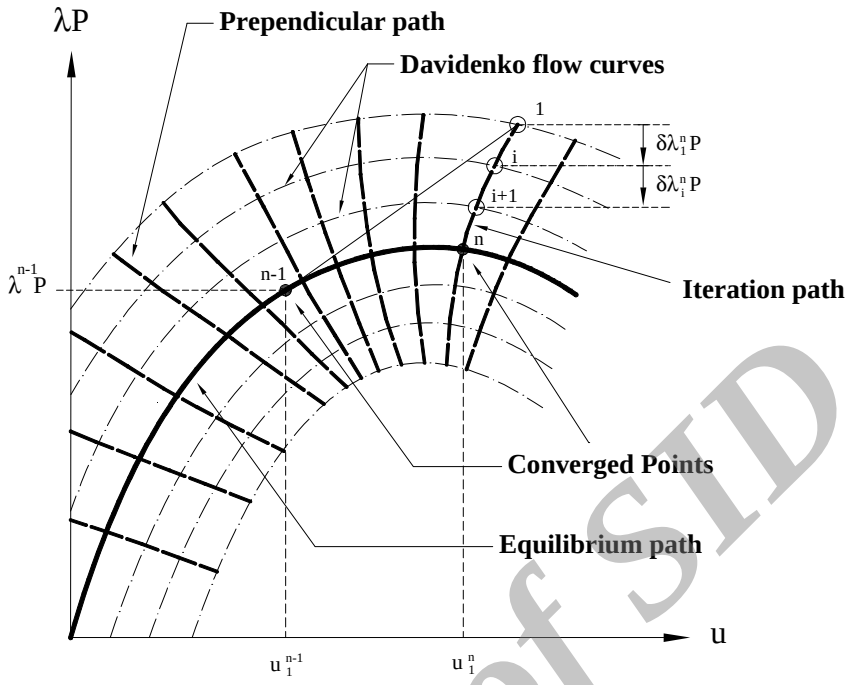

Figure 1. Tracing the equilibrium path utilizing the Davidenko flow curves

$$\delta u_i'^n = \left(K_i^n\right)^{-1} P \tag{7}$$

$$\delta u_i''^n = \left(K_i^n\right)^{-1} R_i^n \tag{8}$$

In these formulations, P and R_i^n are the reference load and the residual load vectors, respectively. K is the stiffness matrix of the structure. Referring to Fig. 2, vector R_i^n is calculated by the following equation representing the difference between the external load applied on structure and the internal force.

$$R_i^n = \lambda_i^n P - F_i^n \tag{9}$$

Vector F_i^n is the internal force of structure. This force is calculated using the following relation at each point, based on the internal stress of structure:

$$F_i^n = \iiint {B_i^n}^T \sigma_i^n \, dV \tag{10}$$

Where, B_i^n is the strain matrix, and σ_i^n is the vector of internal stresses at the i^{th} stage.

In the proposed method, the solution V is replaced with the linear relationship of Batoz and Dhatt. After the selection of various parameters by the authors, the minimum norm answer of Eq.3 is written as follows. It is formulated based on the displacement due to the reference load:

$$\delta u_i^n = V - \frac{V^T \delta u_i'^n}{\left\| \delta u_1'^n \right\|^2} \delta u_i'^n \tag{11}$$

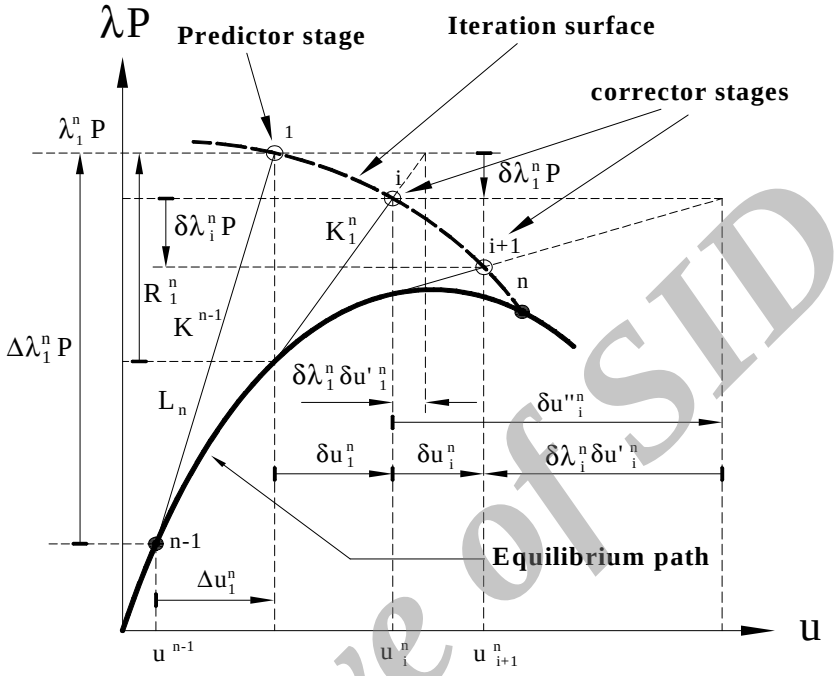

Figure 2. Nonlinear analysis of a structure with one degree of freedom

Where, $\left\| \delta u_1'^n \right\|$ shows the norm of the displacement increment. It is caused by the reference load, in the first iteration. This parameter is employed constantly until the end of the iterative cycles. The load factor increment in the equation of Batoz and Dhatt must be calculated with an arbitrary constraint. In the authors' technique, the constraint of the residual displacement minimization [22] is utilized for finding the load factor increment. Consequently, the equations of V and the load factor increment are expressed in the following forms:

$$V = \delta\lambda_i^n \delta u_i'^n + \delta u_i''^n \tag{12}$$

$$\delta\lambda_i^n = -\frac{\delta u_i''^{nT} \delta u_i'^n}{\delta u_i'^{nT} \delta u_i'^n} \tag{13}$$

In the presented strategy, the load factor increment for tracing the equilibrium path is obtained employing the residual displacement minimization relationship. The displacement and the total load are formulated as follows:

$$u_i^n = u^{n-1} + \Delta u_1^n + \sum_{i=1}^{m} \delta u_i^n \tag{14}$$

$$\lambda^n P = \lambda^{n-1} P + \Delta \lambda_1^n P + \sum_{i=1}^{m} \delta \lambda_i^n P \tag{15}$$

The displacement increment and the load factor increment in the first iteration of each analysis step are indicated by Δu_1^n and $\Delta \lambda_1^n$, respectively. These parameters are shown in Fig. 2. The capability of the suggested approach in tracing the equilibrium path of truss and frame structures, in comparison with other solution methods, will be demonstrated latter. The obtained numerical results indicate that the new solution technique is robust and has good numerical stability, when compared to the other advanced algorithms.

The modified normal flow algorithm was proposed by Saffari et al. in 2008. In this solution scheme, the constraint equation of the residual displacement minimization is used. Therefore, the load factor increment $(\delta\lambda)$ is obtained by Eq.13. In the modified normal flow algorithm, the load factor increment of Eq.13 and the Eq. 12 is employed to compute the particular solution V. Furthermore, the displacement increment in the iterative steps is given by the below formula:

$$\delta u_i^n = V - \frac{V^T \delta u_i'^n}{\left\| \delta u_i'^n \right\|} \delta u_i'^n \tag{16}$$

Notably, the subsequent consideration indicates that the mentioned equation with a little simplification gives the displacement increment of the residual displacement minimization constraint. It should be noted that the two sides of Eq.16 do not have compatible units. This incompatibility is removed by utilizing the exponent of 2 in the denominator of the fraction. Employing Eqs.7, 8, the solution V can be found by Eq.12. The following formulation can be achieved by substituting Eq.12 in Eq.16:

$$\begin{aligned}
\delta u_i^n &= \left(\delta\lambda_i^n \delta u_i'^n + \delta u_i''^n\right) - \frac{\left(\delta\lambda_i^n \delta u_i'^n + \delta u_i''^n\right)^T \delta u_i'^n}{\delta u_i'^{nT} \delta u_i'^n} \delta u_i'^n \\
&= \left(\delta\lambda_i^n \delta u_i'^n + \delta u_i''^n\right) - \frac{\delta\lambda_i^n \delta u_i'^{nT} \delta u_i'^n}{\delta u_i'^{nT} \delta u_i'^n} \delta u_i'^n - \frac{\delta u_i''^{nT} \delta u_i'^n}{\delta u_i'^{nT} \delta u_i'^n} \delta u_i'^n \\
&= \left(\delta\lambda_i^n \delta u_i'^n + \delta u_i''^n\right) - \delta\lambda_i^n \delta u_i'^n - \frac{\delta u_i''^{nT} \delta u_i'^n}{\delta u_i'^{nT} \delta u_i'^n} \delta u_i'^n \\
&= \delta u_i''^n - \frac{\delta u_i''^{nT} \delta u_i'^n}{\delta u_i'^{nT} \delta u_i'^n} \delta u_i'^n
\end{aligned} \tag{17}$$

Clearly, this equation is the displacement increment resulting from the constraint of the

residual displacement minimization method.

3. COMPARISON STUDY

To obtain accurate results, nine solution techniques will be utilized throughout this study. All equilibrium paths of the benchmark problems will be traced with the same load increment assigned at the beginning of the analysis. It is aimed to find the number of complete curve tracings. At the beginning of each analysis, the load factor increment will be given to the computer, as an input data. It is mentioned that the load factor increment is calculated based upon the chord length of the predictor step by the next formula:

$$\Delta\lambda_1^n = \pm\frac{L_n}{\left\|\delta u_1'^n\right\|} \tag{18}$$

In the former equation, $\Delta\lambda_1^n$ is the load increment in the first iteration, and the parameter L_n denotes the chord length of the predictor step. These factors are shown in Fig. 2. It should be noted that for each problem, the chord length of the predictor step is identical for all methods and remains constant throughout the analysis process. As usual, the achieved point from the predictor step returns to the equilibrium path on the iteration surface, by the constraint equation of the solution strategy. Based on these assumptions, only the numerical performances of the constraint equations in returning to the equilibrium path will be compared and evaluated. Some researchers have utilized their techniques by determining the chord length in the first iteration. The generalized displacement control method can be stated as an example [23]. For implementing similar condition for all techniques, the chord length determinations will not be employed throughout this study.

The benchmark problems will be analyzed several times by each strategy. In this regard, maximum allowed iteration, divergence tolerance, maximum and minimum chord length, the number of analyses and the target point are specified. The target point is employed to terminate the solution. This is determined with a specific load factor or a displacement or both. These properties will be given in corresponding tables for each problem. The mentioned parameters will be chosen in such a way that the performance capability of the tactics can be reliably distinguished from each other. The first load factor increment will be calculated as a specific percentage of the first critical load of the equilibrium path. The results of this selection will be obtained after many trials and errors. These parameters will be similar for all approaches. The analysis procedure commences with the minimum arc length and continues to reach the maximum arc length. All the outcomes will be given in the corresponding tables. Convergence criterion used throughout this paper, will be based on the structural residual load, and it will be formulated by the following inequality:

$$R_i^{n^T} R_i^n < \varepsilon \tag{19}$$

The parameter R_i^n indicates the residual force vector in the ith iteration within the nth

analysis step. The factor ε shows the solution tolerance, and it is defined by the analyst. Iterative calculations continue until the convergence criterion will be satisfied. If the number of iterations exceeds the maximum allowed value before satisfying the Eq. 19, the solution is recognized as a diverged one. Other kinds of divergence may occur when the answers go away from the structural equilibrium path. This is known as a jump failure. In this situation, the process cannot trace the correct path.

After identifying the number of converged and diverged analyses, location of the divergence points will be specified in the figures. Therefore, ability or deficiency of the solution techniques becomes clear in passing snap-through and snap-back points. It should be noted that there are a lot of points in the displacement curve, which make the examining of diverged states difficult. To overcome this shortcoming, instead of indicating all diverged points, divergence ranges will be specified. It means that just the points of beginning and end are drawn in each divergence range. Square points illustrated in the figures show the locations that number of negative diagonal arrays of the stiffness matrix changes. For this purpose, the number of negative diagonal arrays of the stiffness matrix will be calculated. When this number is increased or decreased, analysis step is recorded. These are called singular points. It is interesting to note that Huang and Atluri have developed a technique based on the mentioned arrays for tracing post-buckling path of the structures, after bifurcation points [35].

4. NUMERICAL EXAMPLES

In order to present the efficiency and reliability of the proposed method, some benchmark structures with severe nonlinear behaviors will be analyzed in this part. The criteria of the comparison are selected in such a way that the various aspects of the techniques' abilities can be accurately evaluated and compared. In fact, the number of complete tracings of the equilibrium path illustrates the ability to traverse the snap-through and snap-back points. The tables of results clarify the numerical stability of the suggested approach in passing the load limit and snap-back points. For simplicity, the short form of the methods' name is used throughout the article. Table 1 shows the complete and abbreviation name of the solution techniques. The authors' approach is shown by RDI.

Table 1: Short form of the solution technique

Row	Solution Technique	Short Form
1	Residual Load Minimization	RLM
2	Normal Plane	NP
3	Updated Normal Plane	UNP
4	Cylindrical Arc Length	CAL
5	Work Control	WC
6	Residual Displacement Minimization	RDM
7	Generalized Displacement Control	GDC
8	Modified Normal Flow	MNF
9	Robust Displacement Increment	RDI

4.1 Example one

Fig. 3 illustrates a three-member truss, which has three pinned supports. This structure has four nodes and two degrees of freedom. The tip node is subjected to horizontal and vertical point loads ($P=10000\,\mathrm{N}$). Axial rigidity of the members is $AE=2\times10^{5}\,\mathrm{N}$. Fig. 4 shows the load-displacement curve of structure for vertical degree of freedom (u).

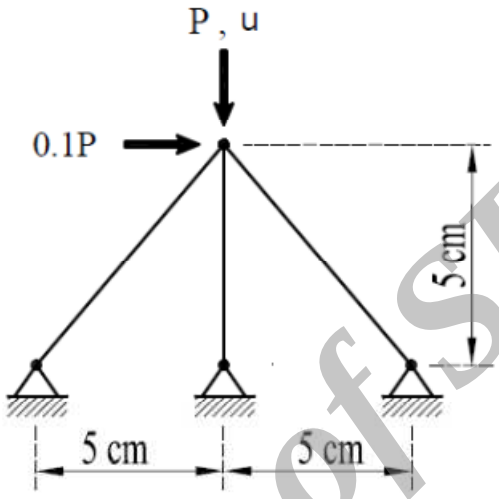

Figure 3. Three-member truss

Table 2: Analysis properties of the three-member truss

Max. of Iteration	Tolerance for Conv.	Arc Length		Target Point		
		Minimum	Increment	Num. of analyses	Load Factor	Displacement
5	1×10^{-4}	0.250	0.015	45	-18.11	-5.9

Table 3: Numerical results of the three-member truss

Analysis Method	Number of Analyses	Number of Convergences	Number of Failures	Number of Jumps	Convergence Percentage
RLM	45	31	2	12	68.89
NP	45	29	11	5	64.44
UNP	45	35	5	5	77.78
CAL	45	43	2	0	95.56
WC	45	0	45	0	0
RDM	45	45	0	0	100
GDC	45	6	39	0	13.33
MNF	45	45	0	0	100
RDI	45	45	0	0	100

Table.3 indicates that the residual displacement minimization, the modified normal flow and the suggested techniques have entirely traced the equilibrium path in all analyses. These are the superior procedures. Constant work control strategy failed in all the solutions. Other results are presented in the corresponding table.

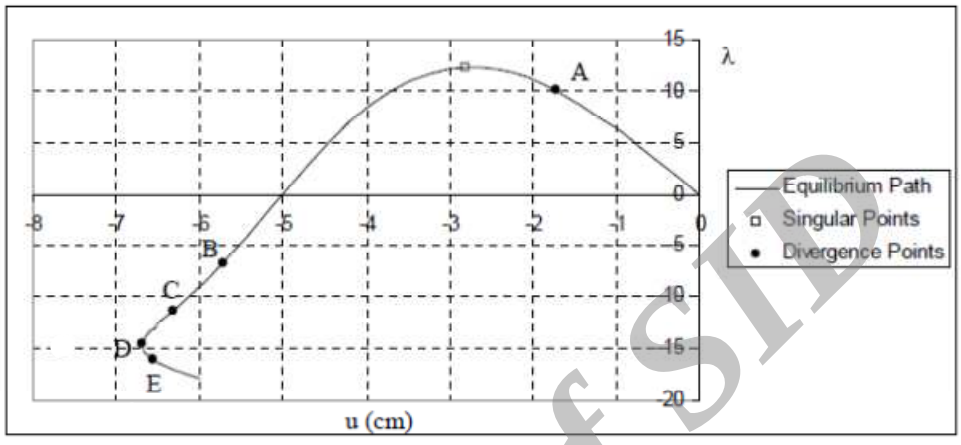

Figure 4. Equilibrium path of the three-member truss

As it is shown in Fig. 4, the behavior of this structure has the load, and displacement limit points. The residual load minimization method diverged in point A and in the range of EF. This technique presents poor performance in passing the load limit points. The constant work control procedure diverged before the snap-back point and in the interval BD. The diverged analyses of the generalized displacement control method are located in BE. Cylindrical arc length, updated normal plane, residual displacement minimization and the modified normal flow strategies diverged in the range DE. The diverged analyses of the normal plane method occurred in CE.

4.2 Example two

The arch truss, shown in Fig. 5, is subjected to a vertical downward point load of 10 kN at its tip. Arch's radius of the truss is $R = 48cm$. Axial rigidity of the members is identical and is considered to be $EA = 50MN$. The load-deflection curve of this structure for degree of freedom u is given in Fig. 23. It should be noted that this truss was investigated by other researchers, as well [36-38].

Table 4: Analysis properties of 101-member arch truss

Max. of Iteration	Tolerance for Conv.	Arc Length			Target Point	
		Minimum	Increment	Num. of Increments	Load Factor	Displacement
8	1×10^{-5}	0.01	0.0005	120	200	NA

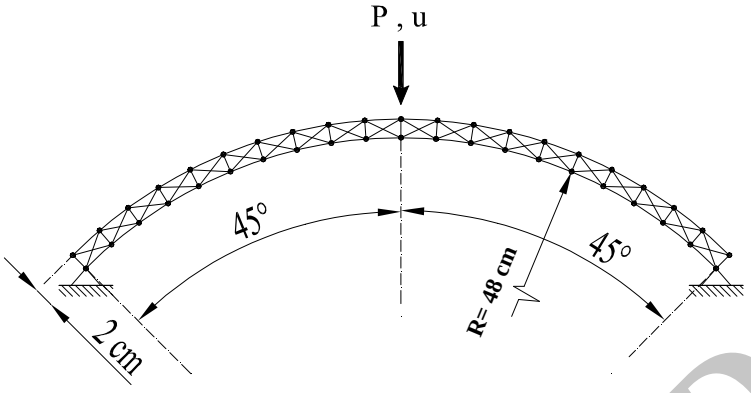

Figure 5. 101-member arch truss

Table 5: Numerical results of 101-member arch truss

Analysis Method	Number of Analyses	Number of Convergences	Number of Failures	Number of Jumps	Convergence Percentage
RLM	120	0	0	120	0
NP	120	44	24	52	36.67
UNP	120	90	3	27	75
CAL	120	62	55	3	51.67
WC	120	0	75	45	0
RDM	120	93	2	25	75.5
GDC	120	6	17	97	5
MNF	120	7	99	14	5.83
RDI	120	94	0	26	78.33

As it is shown in Fig. 6, the load-displacement curve of this structure has two load limit points and two displacement limit points. The proposed strategy is the most efficient technique, and it could completely trace the equilibrium path in 78 percent of all solutions.

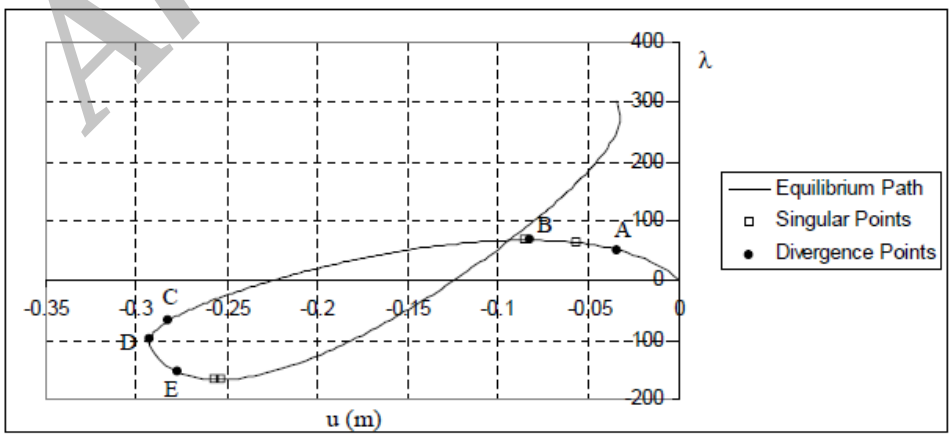

Figure 6. Equilibrium path of 101-member arch truss

The residual load minimization method jumped over the equilibrium path in range of AB. The diverged analyses of the work control and the normal plane approaches are located in CD and CE, respectively. The updated normal plane, the cylindrical arc length, the residual displacement minimization and the modified normal flow methods and also the suggested technique diverged in the range of DE. It should be noted that the residual load minimization tactic returns on the equilibrium path after reaching the first load limit point in all analyses. It is obvious that this approach faces difficulties in the snap-through points.

4.3 Example 3

The truss structure shown in Fig. 7 is subjected to the asymmetrical loading. On the other hand, the geometry of the structure is also asymmetric. These characteristics result in intense nonlinear behavior in the load-displacement curve. This bridge has 33 members and 32 degrees of freedom. The cross section areas of all members are $A=3cm^2$. The modulus of elasticity is $E=3\times10^4\ kN/cm^2$. The nonlinear behavior of this bridge is studied for the degree of freedom u. Fig. 8 illustrates the equilibrium path. Previously, Powell and Simons [8] and also Saffari et al. [24] analyzed this structure.

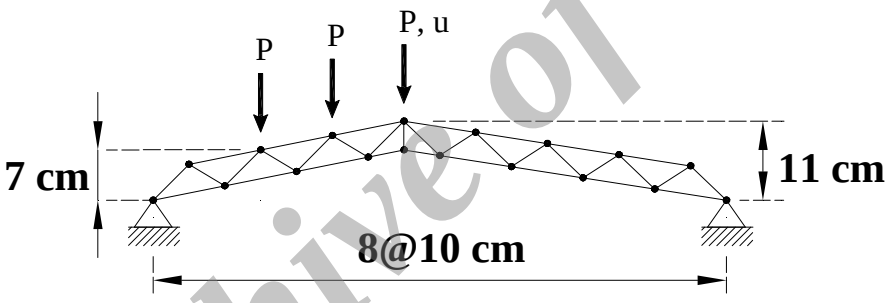

Figure 7. 33-member truss bridge

Table 6: Analysis properties of the 33-member truss bridge

Max. of Iteration	Tolerance for Conv.	Arc Length		Num. of analyses	Target Point	
		Minimum	Increment		Load Factor	Displacement
5	1×10^{-5}	5	0.05	300	NA	150

Table 7: Numerical results of the 33-member truss bridge

Analysis Method	Number of Analyses	Number of Convergences	Number of Failures	Number of Jumps	Convergence Percentage
RLM	300	0	300	0	0
NP	300	170	130	0	56.67
UNP	300	197	103	0	65.67
CAL	300	222	78	0	74
WC	300	0	300	0	0
RDM	300	200	100	0	66.67

GDC	300	94	206	0	31.33
MNF	300	0	300	0	0
RDI	300	206	94	0	68.67

Referring to Fig. 8, several snap-through and snap-back points are seen in the load-displacement path. Based on Table.7, the Crisfield arc length scheme and the suggested technique have the highest convergence efficiency. On the other hand, the work control and the modified displacement control solution procedures did not completely trace the curve.

According to Fig. 8, all analyses of the residual load minimization method diverged in AB. This method could trace the equilibrium path before reaching the load limit point. The diverged solutions of the normal plane, the work control and the generalized displacement control techniques occurred within the range of CD. The diverged analyses of residual displacement minimization algorithm and the proposed technique situate in point E.

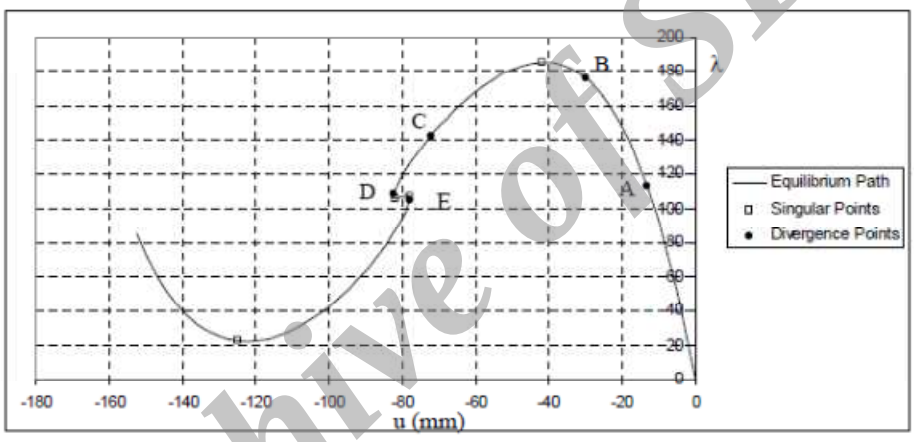

Fig. 8. Equilibrium path of the 33-member truss bridge

4.4 Example four

The arch frame shown in Fig. 9 is subjected to a point of load $P=1\,\mathrm{N}$ with an eccentricity of 200. The span and height of the frame are 10000 and 500, respectively. 12 identical elements have been used to model the structure. There are hinged on the structural supports at its two ends. Fig. 10 displays the nonlinear behavior of the frame for the vertical nodal degree of freedom under the point load. The cross section area, the second moment of area and Young's modulus of elasticity are $A=1$, $I=1$ and $E=200$, respectively. Harrison analyzed this structure using the discrete element tactic [34]. Other researchers also studied this frame [40-42].

Table 8: Analysis properties of shallow arch frame

Max. of Iteration	Tolerance for Conv.	Arc Length		Target Point		
		Minimum	Increment	Num. of analyses	Load Factor	Displacement
20	1×10^{-4}	20	0.5	100	NA	1000

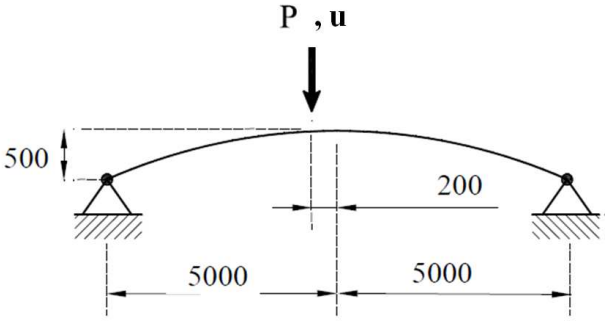

Figure 9. Shallow arch frame

Table 9: Numerical results of shallow arch frame

Analysis Method	Number of Analyses	Number of Convergences	Number of Failures	Number of Jumps	Convergence Percentage
RLM	100	0	100	0	0
NP	100	73	27	0	73
UNP	100	58	36	6	58
CAL	100	75	25	0	75
WC	100	0	100	0	0
RDM	100	94	6	0	94
GDC	100	17	83	0	17
MNF	100	0	100	0	0
RDI	100	97	3	0	97

Fig. 10 shows the complex behavior of this structure with the snap-through and snap-back points. The mentioned nonlinear algorithms are evaluated by performing 100 analyses. Among them, the suggested technique has the best outcomes with 97 converged solutions. The residual load minimization, the constant work control and the modified work control methods failed before the target point in all analyses. The results are given in Table.9.

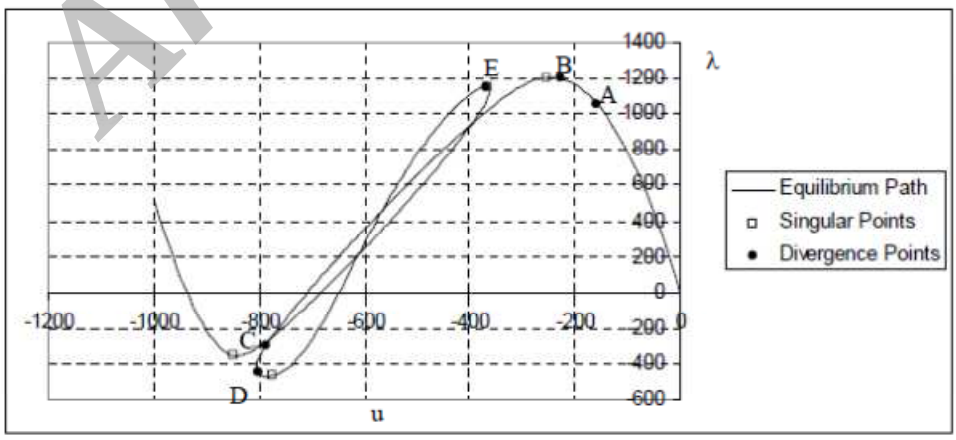

Figure 10. Equilibrium path of Shallow arch frame

Based on Fig. 10, the residual load minimization method diverged in domain AB. All analyses of this approach failed to make forward progress before the load limit point. The constant work control method diverged in the region CD. The diverged analyses of the normal plane, and the generalized displacement control techniques occurred at points E and D. The updated normal plane, the cylindrical arc length, the residual displacement minimization, the modified normal flow and the proposed methods diverged in point D.

4.5 Example five

The frame of Fig. 11 was studied by Harrison [39]. Yung et al. have also analyzed this structure [23, 35]. The arch radius is $R=127\,\text{cm}$ $(R=50\,\text{in})$. The modulus of elasticity and the second moment of inertia are $E=1378\,\text{kPa}$ $(E=200\,\text{psi})$ and $I=41.62\,\text{cm}^4$ $(I=1\,\text{in}^4)$, respectively. Moreover, the cross section area of the member is considered to be $A=64.5\,\text{cm}^2$ $(A=10\,\text{in}^2)$. The structure is divided into 26 equal elements. According to Fig. 11, this structure is subjected to a point load ($P=1\,\text{N}$) with eccentricity of $\text{b}=7.98\,\text{cm}$ $(\text{b}=3.14\,\text{in})$. The load-displacement curve for the vertical direction of the top node (V) is presented in Fig. 12.

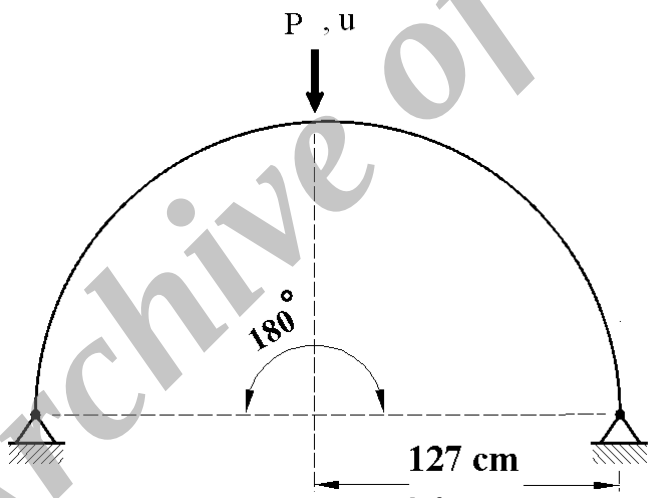

Figure 11. Deep arch frame

Table 10: Analysis properties of deep arch frame

Max. of Iteration	Tolerance for Conv.	Arc Length		Num. of analyses	Target Point	
		Minimum	Increment		Load Factor	Displacement
8	1×10^{-4}	5	0.1	40	1.75	-22.6

Table 11: Numerical results of the deep arch frame

Analysis Method	Number of Analyses	Number of Convergences	Number of Failures	Number of Jumps	Convergence Percentage
RLM	40	0	40	0	0
NP	40	27	13	0	67.5
UNP	40	21	19	0	52.5
CAL	40	26	14	0	65
WC	40	0	40	0	0
RDM	40	27	13	0	67.5
GDC	40	2	38	0	5
MNF	40	0	40	0	0
RDI	40	40	0	0	100

Referring to Fig. 12, the equilibrium path of the deep arch frame has several snap-through and snap-back points. In this problem, the proposed method has the best performance and could completely trace the path in all analyses. The residual load minimization and the constant work control techniques diverged in all analyses. Table 11 indicates the numerical results.

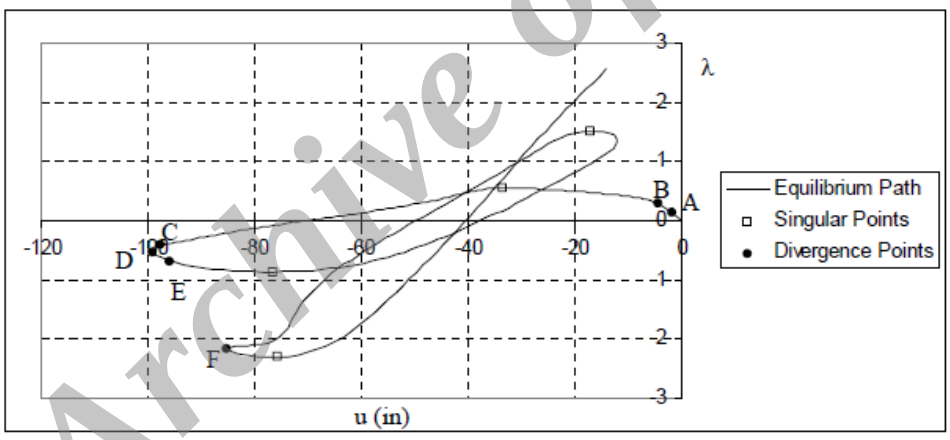

Figure 12. Equilibrium path of the deep arch frame

All solutions of the load minimization and the constant work control methods diverged in ranges AB and CD, respectively. Some of the analyses of the generalized displacement control approach failed to converge in region DE and some other at the point F. The diverged solutions of the normal plane, the updated normal plane and the cylindrical arc length techniques occurred in point F. Consequently; the last three methods traced a longer path before reaching the divergence point.

5. CONCLUSION

In this paper, a displacement increment was proposed for geometrically nonlinear structural analysis. This approach can be employed with the various constraints for calculating the load factor. According to the numerical results, the authors' method can trace the equilibrium path of the structures with severe nonlinear behavior. The advantage of the presented algorithm was illustrated in the comparison with eight advanced solution techniques, including residual load minimization, normal plane, updated normal plane, cylindrical arc length, work control, residual displacement minimization, generalized displacement control and modified normal flow. To examine the suggested approach qualifications, five benchmark truss and frame problems were solved. These structures were analyzed more than 5000 times. The numerical outcomes indicated high capability and reliability of the proposed strategy in passing the load limit and snap-back points. As it was demonstrated numerically, the presented procedure has numerical stability in the structural analysis. Fig. 13 shows the total result of performed analyses. This bar chart presents the percentage of the fully traced equilibrium path, in which no fail or jump was occurred.

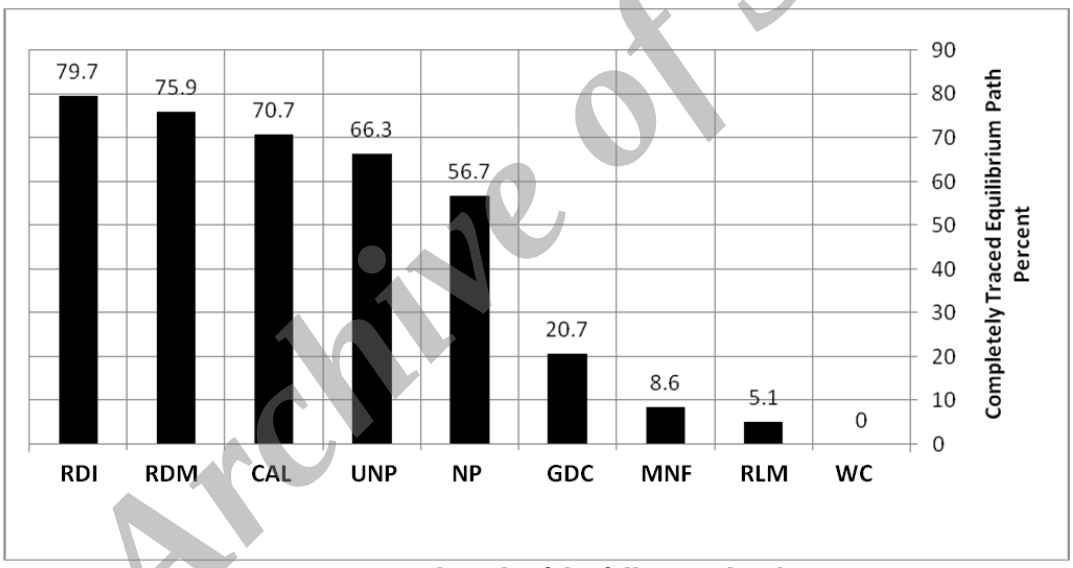

Figure 13. Total result of the fully traced paths

REFERENCES

1. Zienkiewicz OC, Taylor RL. *The Finite Element Method for Solid and Structural Mechanics*, Butterworth-Heinemann, 2005.
2. Waszczyszyn Z, Cichoń Cz, Radwańska M. *Stability of Structures by Finite Element Methods*, Elsevier, Amsterdam, 1994.
3. Argyris JH. Continua and discontinua, *Proceedings of First Conference on Matrix Methods in Structural Mechanics, Wright-Patterson Air Force Base*, Ohio, 1965, pp. 11-89.
4. Batoz J, Dhatt G. Incremental displacement algorithms for nonlinear problems,

International Journal for Numerical Methods in Engineering, **14**(1979) 1262-67.
5. Zienkiewicz OC. Incremental displacement in non-linear analysis, *International Journal for Numerical Methods in Engineering*, **3**(1971) 587-92.
6. Pian THH, Tong P. Variational formulation of finite displacement analysis, B.F. de Veubeke (Eds.), *Proceedings of IUTAM Symposium on High Speed Computing of Elastic Structures*, University of Liege, Liege, Belgium, 1971, pp. 43-63.
7. Ramm E. *Strategies for Tracing the Nonlinear Response Near Limit Points*, W. Wunderlich, E. Stein and K.J. Bathe (Eds.), nonlinear finite element analysis in structural mechanics, Springer, Berlin, 1981, pp. 63-89.
8. Powell G, Simons J. Improved iteration strategy for nonlinear structures, *International Journal for Numerical Methods in Engineering*, **17**(1981) 1455-67.
9. Bergan PG, Soreide TH. *Solution of Large Displacement and Instability Problems Using the Current Stiffness Parameters*, in: P.G. Bergan et al. (Eds.), Finite Elements in Nonlinear Mechanics, Tapir, **2**(1978) 647-69.
10. Crisfield M. A fast incremental/iterative solution procedure that handles "snap-through", *Computers and Structures*, **13**(1981) 55-62.
11. Waszczyszyn Z. Numerical problems of nonlinear stability analysis of elastic structures, *Computers and Structures*, **17**(1983) 13-24.
12. Bergan P. Solution algorithms for nonlinear structural problems, *Computers and Structures*, **12**(1980) 497-509.
13. Wempner GA. Discrete approximations related to nonlinear theories of solids, *International Journal of Solids and Structures*, **7**(1971) 1581-9.
14. Riks E. The application of Newton's method to the problem of elastic stability, *Journal of Applied Mechanics*, **39**(1972) 1060-5.
15. Riks E. An incremental approach to the solution of snapping and buckling problems, *International Journal of Solids and Structures*, **15**(1979) 529-51.
16. Rezaiee-Pajand M, Tatar M. Modified arc length method for nonlinear structural analysis, *Technical and Engineering Journal of Shahid Chamran University*, Ahvaz, Iran, **5**(2005) 71-86. (in Persian)
17. Rezaiee-Pajand M, Akhaveysi A.H. Ellipsoidal arc length method, *Proceedings of 5th International Conference on Civil Engineering*, Ferdowsi University, Mashhad, Iran, Vol. 2, 2000, pp. 402-10. (in Persian)
18. Sousa CAG, Pimenta PM. A new parameter to arc-length method in nonlinear structural analysis, Asociación argentina de mecánica computacional, *Structural Mechanics*, **29**(2010) 1841-8.
19. Hinton E, Owen DRJ, Taylor C. *Recent Advances in Non-Linear Computational Mechanics*, Pineridge Press Limited, 1982.
20. Forde B, Stiemer S. Improved arc length orthogonality methods for nonlinear finite element analysis, *Computers and Structures*, **27**(1987) 625-30.
21. Yang YB, McGuire W. A work control method for geometrically nonlinear analysis, *Proceedings of International Conference on Numerical Methods in Engineering: Theory and Applications*, J. Middleton and G.N. Pande (Eds.), University College Swansea, Wales, UK, 1985, pp. 913-921.
22. Chan SL. Geometric and material non-linear analysis of beam-columns and frames using the minimum residual displacement method, *International Journal for Numerical*

Methods in Engineering, **26**(1988) 2657-69.
23. Yang Y, Shieh M. Solution method for nonlinear problems with multiple critical points, *AIAA Journal*, **28**(1990) 2110-6.
24. Saffari H, Fadaee M, Tabatabaei R. Nonlinear analysis of space trusses using modified normal flow algorithm, *Journal of Structural Engineering*, **134**(2008) 998-1005.
25. Watson LT, Billups SC, Morgan AP. Algorithm 652: Hompack: a suite of codes for globally convergent homotopy algorithms, *ACM Transactions on Mathematical Software*, **13**(1987) 281-310.
26. Watson LT, Sosonkina M, Melville RC, Morgan AP, Walker HF. Algorithm 777: Hompack90: a suite of Fortran 90 codes for globally convergent homotopy algorithms, *ACM Transactions on Mathematical Software*, **23**(1997) 514–9.
27. Saffari H, Mansouri I. Non-linear analysis of structures using two-point method, *International Journal of Non-Linear Mechanics*, **46**(2011) 834-40.
28. Mansouri I, Saffari H. An efficient nonlinear analysis of 2D frames using a Newton-like technique, *Archives of Civil and Mechanical Engineering*, **12**(2012) 485-92.
29. Rezaiee-Pajand M, Ghalishooyan M, Salehi-Ahmadabad M. Comprehensive evaluation of structural geometrical nonlinear solution techniques, Part I: Formulation and characteristics of the methods, *Structural Engineering and Mechanics*, **48**(2013) 849-78.
30. Rezaiee-Pajand M, Ghalishooyan M, Salehi-Ahmadabad M. Comprehensive evaluation of structural geometrical nonlinear solution techniques, Part II: Comparing efficiencies of the methods, *Structural Engineering and Mechanics*, **48**(2013) 879-914.
31. Phung-Van P, Nguyen-Thoi T, Luong-Van H. Lieu-Xuan Q. Geometrically nonlinear analysis of functionally graded plates using a cell-based smoothed three-node plate element (CS-MIN3) based on the C0-HSDT, *Computer Methods in Applied Mechanics and Engineering*, **270**(2014) 15–36.
32. Watson LT, Holze SM, Hansen M.C. *Tracking Nonlinear Equilibrium Paths by A Homotopy Method*, Technical Report. No. CS81001-R, Virginia Polytechnic Institute and Blacksburg University, 1981, pp. 1–21.
33. Allgower EL, Georg K. *Homotopy Methods for Approximating Several Solutions to Nonlinear Systems of Equations, Numerical Solution of Highly Nonlinear Problems*, W. Forster, (Eds.), North-Holland, Amsterdam, The Netherlands, 1980, pp. 253–270.
34. Zienkiewicz OC. *The Finite Element Method*, third ed., McGraw-Hill, London, 1977.
35. Huang BZ, Atluri SN. A simple method to follow post-buckling paths in finite element analysis, *Computers and Structures*, **57**(1995) 477-89.
36. Crisfield MA. *Non-Linear Finite Element Analysis of Solids and Structures*: Vol. 2: Advanced Topics, John Wiley & Sons, 1997.
37. Kim JH, Kim YH. A predictor-corrector method for structural nonlinear analysis, *Computer Methods in Applied Mechanics and Engineering*, **191**(2001) 959-74.
38. Hrinda GA. *Geometrically Nonlinear Static Analysis of 3D Trusses Using the Arc-Length Method*, in Computational Methods and Experimental Measurements XIII, Prague, Czech Republic, (2007) 243-52.
39. Harrison H. *Elastic Post-Buckling Response of Plane Frames*, in: L.J. Morris (Eds.), Instability and Plastic Collapse of Steel Structures, Granada, 1983, pp. 56-65.
40. Yang YB, Kuo SR. *Theory and Analysis of Nonlinear Framed Structures*, Singapore, Prentice Hall, 1994.

41. Clarke MJ, Hancock GJ. A study of incremental-iterative strategies for non-linear analyses, *International Journal for Numerical Methods in Engineering*, **29**(1990) 1365-91.
42. Rezaiee-Pajand M, Tatar M, Moghaddasie B. Some geometrical bases for incremental-iterative methods, *International Journal of Engineering*, Transactions B: Applications, **22**(2009) 245-56.